




 Cite this: *RSC Adv.*, 2020, 10, 29835

# Microwave dielectric properties of low-temperature-fired $\text{MgNb}_2\text{O}_6$ ceramics for LTCC applications

 Chenghao Wu,<sup>a</sup> Yongda Hu,<sup>a</sup>  Shengxiang Bao,<sup>a</sup> Gang Wang,<sup>a</sup>  Pengbo Jiang,<sup>a</sup> Jie Chen,<sup>b</sup> Zongzhi Duan<sup>b</sup> and Wenhui Deng<sup>a</sup>

$\text{MgNb}_2\text{O}_6$  ceramics doped with  $(\text{Li}_2\text{O}-\text{MgO}-\text{ZnO}-\text{B}_2\text{O}_3-\text{SiO}_2)$  glass were synthesized by the traditional solid phase reaction route. The effects of LMZBS addition on microwave dielectric properties, grain growth, phase composition and morphology of  $\text{MgNb}_2\text{O}_6$  ceramics were studied. The SEM results show dense and homogeneous microstructure with grain size of 1.72  $\mu\text{m}$ . Raman spectra and XRD patterns indicate the pure phase  $\text{MgNb}_2\text{O}_6$  ceramic. The experimental results show that LMZBS glass can markedly decrease the sintering temperature from 1300 °C to 925 °C. Higher density and lower porosity make ceramics have better dielectric properties. The  $\text{MgNb}_2\text{O}_6$  ceramic doped with 1 wt% LMZBS glass sintered at 925 °C for 5 h, possessed excellent dielectric properties:  $\epsilon_r = 19.7$ ,  $Q \cdot f = 67\,839$  GHz,  $\tau_f = -41.01$  ppm °C<sup>-1</sup>. Moreover, the favorable chemical compatibility of the  $\text{MgNb}_2\text{O}_6$  ceramic with silver electrodes makes it as promising material for low temperature co-fired ceramic (LTCC) applications.

 Received 13th June 2020  
 Accepted 6th August 2020

DOI: 10.1039/d0ra05211f

[rsc.li/rsc-advances](http://rsc.li/rsc-advances)

## 1. Introduction

The forward evolution of electronics, power systems, satellite broadcasting and wireless communication,<sup>1</sup> especially the rapid development of 5G communication, have posed great demands for high integration and miniaturization.<sup>2,3</sup> And considering their excellent microwave dielectric properties, microwave dielectric materials have attracted more attention in passive electronic components, such as dielectric resonators, filters and other devices.<sup>4,5</sup> Additionally, LTCC technology is favored by advanced products because of their high demands for miniaturization and hybrid integration for electronic systems. For instance, Guo *et al.*<sup>44–46</sup> successfully lowered the sintering temperature of ceramics by ions substitution and addition of low melting point oxide. In order to co-fire with silver electrode, ceramics must be synthesized at low temperature, less than 960 °C.<sup>6,7</sup> Hence, the aim of the present work is to decrease the sintering temperature of  $\text{MgNb}_2\text{O}_6$  ceramics and then achieve excellent chemical compatibility with silver for the first time to satisfy the demands for LTCC applications. Generally, the sintering temperature of ceramic materials can be effectively reduced by the following methods: (1) use the raw materials with lower melting temperature, such as  $\text{Bi}_2\text{Mo}_2\text{O}_9$  ceramics.<sup>8</sup> (2) Use ultrafine powders as raw materials to decrease the densification temperature.<sup>9</sup> (3) Adopt proper synthesis process,

such as co-precipitation, sol-gel and hydrothermal methods.<sup>10,11</sup> (4) Use reasonable ion substitution.<sup>12,13</sup> (5) Select appropriate low-melting glass or oxide to reduce the sintering temperature. The commonly used low-melting glasses are  $\text{PbO}-\text{Bi}_2\text{O}_3-\text{B}_2\text{O}_3-\text{ZnO}-\text{TiO}_2$ ,  $\text{B}_2\text{O}_3-\text{CuO}$ ,  $\text{Li}_2\text{O}-\text{B}_2\text{O}_3-\text{SiO}_2-\text{CaO}-\text{Al}_2\text{O}_3$ .<sup>14,15</sup>

Binary magnesium niobate ceramics with rhombic columnar structure are widely investigated because of their excellent microwave dielectric properties.<sup>16,17</sup> However, the pure phase  $\text{MgNb}_2\text{O}_6$  ceramic is not easy to obtain, as reported by Liou *et al.*<sup>18</sup> Pullar *et al.*<sup>19</sup> reported that  $\text{MgNb}_2\text{O}_6$  ceramic sintered at 1300 °C for 2 h exhibited remarkable microwave properties:  $\epsilon_r = 19.9$ ,  $Q \cdot f = 79\,600$  GHz,  $\tau_f = -64.9$  ppm °C<sup>-1</sup>. Tian *et al.*<sup>20</sup> reported that  $\text{MgNb}_2\text{O}_6$  ceramic were not only successfully sintered at 1050 °C, but also achieved remarkable microwave properties:  $\epsilon_r = 21.5$ ,  $Q \cdot f = 108\,000$  GHz,  $\tau_f = -44$  ppm °C<sup>-1</sup> by adding  $\text{CuO}-\text{B}_2\text{O}_3$  as sintering aid. However, the sintering temperature is still too high.

As known, the synthesis of pure-phase  $\text{MgNb}_2\text{O}_6$  ceramics is not easy.<sup>23</sup> In this work, pure-phase  $\text{MgNb}_2\text{O}_6$  ceramic was synthesized successfully by optimizing process parameters. Such as, the slightly excessive MgO, reasonable extension of the milling time and increase in the pre-sintering time. George, Sumesh, *et al.*<sup>44</sup> reported that the addition of LMZBS glass decreased the sintering temperature of  $\text{Li}_2\text{MgSiO}_4$  ceramics from 1250 to 875 °C. Besides, the LMZBS glass melts to form a liquid phase and wet the grains of  $\text{MgNb}_2\text{O}_6$ , thereby promoting the densification of  $\text{MgNb}_2\text{O}_6$ .<sup>44</sup> In addition, magnesium oxide in LMZBS glass can compensate for the volatilization of MgO in  $\text{MgNb}_2\text{O}_6$ , so LMZBS glass plays

<sup>a</sup>University of Electronic Science and Technology of China, Chengdu, 610054, China.  
 E-mail: 3097213743@qq.com

<sup>b</sup>Chengdu Yaguang Electronics Co. Ltd., Microwave Circuit & System Institute, Chengdu, 610054, China



a great role in low-temperature sintering. In the present work, we have chosen LMZBS glasses as the firing aid to reduce the sintering temperature of  $\text{MgNb}_2\text{O}_6$  ceramics. To our best knowledge, there's been no relevant report about the co-fired experiment of  $\text{MgNb}_2\text{O}_6$  ceramics with silver electrodes. In this work, the chemical compatibility of  $\text{MgNb}_2\text{O}_6$  ceramics with Ag electrodes have been studied for the first time. Meanwhile, the effects of LMZBS glass addition on the microstructure, density and dielectric properties of  $\text{MgNb}_2\text{O}_6$  ceramics were also studied.

## 2. Experimental procedures

### 2.1. Materials preparation

$\text{MgNb}_2\text{O}_6$  ceramics were synthesized by solid-state process using high-purity MgO and  $\text{Nb}_2\text{O}_5$  (all purity > 99.9%) as original materials were. The stoichiometric ratio of MgO and  $\text{Nb}_2\text{O}_5$  was 1.01 : 1. (The slightly excessive MgO is beneficial to inhibit the production of the secondary phases  $\text{Mg}_4\text{Nb}_9\text{O}_{24}$  and  $\text{Nb}_2\text{O}_5$ <sup>24,25</sup>). The powders were milled for 24 h, dried, and finally calcined at 1000 °C for 8 h. (An appropriate increase in the pre-sintering time is conducive to the formation of single-phase  $\text{MgNb}_2\text{O}_6$  ceramic, and a reasonable extension of the milling time will increase the uniformity of particles and decrease particle size<sup>23,26</sup>).  $\text{Li}_2\text{O}$ - $\text{MgO}$ - $\text{ZnO}$ - $\text{B}_2\text{O}_3$ - $\text{SiO}_2$  (LMZBS) glass was synthesized by quenching method according to the mole percentage of:  $\text{Li}_2\text{CO}_3$  :  $\text{MgO}$  :  $\text{ZnO}$  :  $\text{B}_2\text{O}_3$  :  $\text{SiO}_2$  = 20 : 20 : 20 : 20 : 20 (all purity > 99%). The LMZBS glass<sup>21,22</sup> was melted and quenched at 900 °C. Then different weight percentages of LMZBS glasses ( $x$  = 0.1 wt%, 0.5 wt%, 1 wt%, 1.5 wt%, 2 wt%) were added to the calcined  $\text{MgNb}_2\text{O}_6$  powders. After the second ball-milling for 12 h, the mixtures were dried, mixed with 10% PVB and then pressed into small cylinders 12 mm in diameter and 6 mm in height. Ultimately, the pressed cylinders pellets were sintered at 850–950 °C for 5 h.

### 2.2. Characterization analysis

The bulk density of all samples was measured by Archimedes method. The phase composition and crystal structure were analyzed by X-ray diffractometer (Philips X'Pert Pro MPD, The Netherlands). The scanning angle was ranged from 20° to 70°. The operating voltage and current of Cu K $\alpha$  radiation were 40 kV and 30 mA, respectively. Raman spectroscopy was used to analyze (InVia, Renishaw, UK) the crystal structure of  $\text{MgNb}_2\text{O}_6$  ceramic. The microstructure was studied detailed by scanning electron microscope (SEM, JSM-6490LV; JEOL, Japan).<sup>27</sup> Moreover, the distribution of elements was collected by X-ray spectrometer (EDX, Genesis; EDAX, USA). The dielectric constant ( $\epsilon_r$ ) and quality factor ( $Q \cdot f$ )<sup>28</sup> were calculated by a network analyzer (N5230A, USA) combining the resonant cavity method and the Hakki-Coleman method in TE011 mode. The resonant frequency temperature coefficient ( $\tau_f$ ) was calculated as follows:<sup>29</sup>

$$\tau_f = \frac{f_2 - f_1}{f_1 \times (t_2 - t_1)} \quad (1)$$

where  $t_1$  = 25 °C and  $t_2$  = 85 °C, corresponding resonance frequencies are  $f_{t_1}$  and  $f_{t_2}$ , respectively.

## 3. Results and discussion

### 3.1. Crystal structure and phase composition

Fig. 1 indicates the XRD patterns of the  $\text{MgNb}_2\text{O}_6$  ceramics with different LMZBS additions sintered at 925 °C for 5 h. All the ceramics samples show an orthorhombic columbite structure  $\text{MgNb}_2\text{O}_6$  phase (PDF file no. 88-0708). By comparing the diffraction peaks with the standard PDF card, no second phase was found within the measurement error range of the instrument, indicating that pure phase  $\text{MgNb}_2\text{O}_6$  ceramics were formed through slightly excessive MgO in the synthesis process and LMZBS glass had no significant effect on phase composition for  $\text{MgNb}_2\text{O}_6$  ceramics.

Fig. 2 shows the Raman spectra of  $\text{MgNb}_2\text{O}_6$  ceramics at 925 °C. Raman spectral is often used to study the crystal structure of materials. According to the symmetry of crystal, the

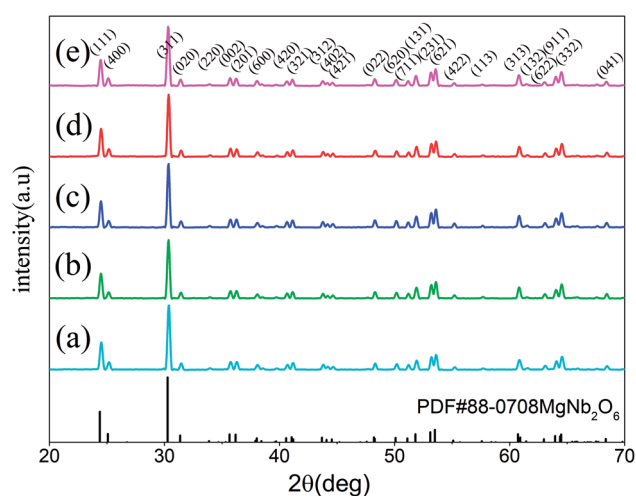


Fig. 1 XRD patterns of  $\text{MgNb}_2\text{O}_6$ - $x$  wt% LMZBS ceramics sintered at 925 °C for 5 h: (a)  $x$  = 0.1, (b)  $x$  = 0.5, (c)  $x$  = 1.0, (d)  $x$  = 1.5, and (e)  $x$  = 2.0.

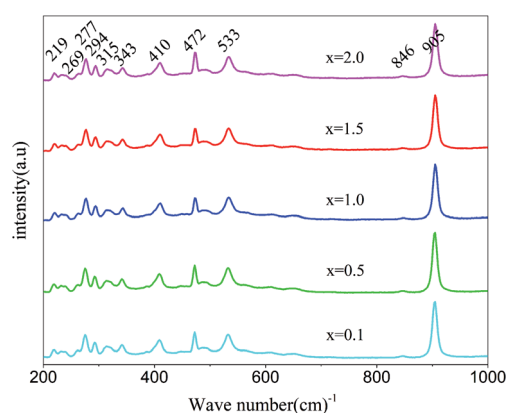


Fig. 2 Raman spectra of the  $\text{MgNb}_2\text{O}_6$ - $x$  wt% LMZBS ( $x$  = 0.1–2.0) ceramics sintered at 925 °C for 5 h.



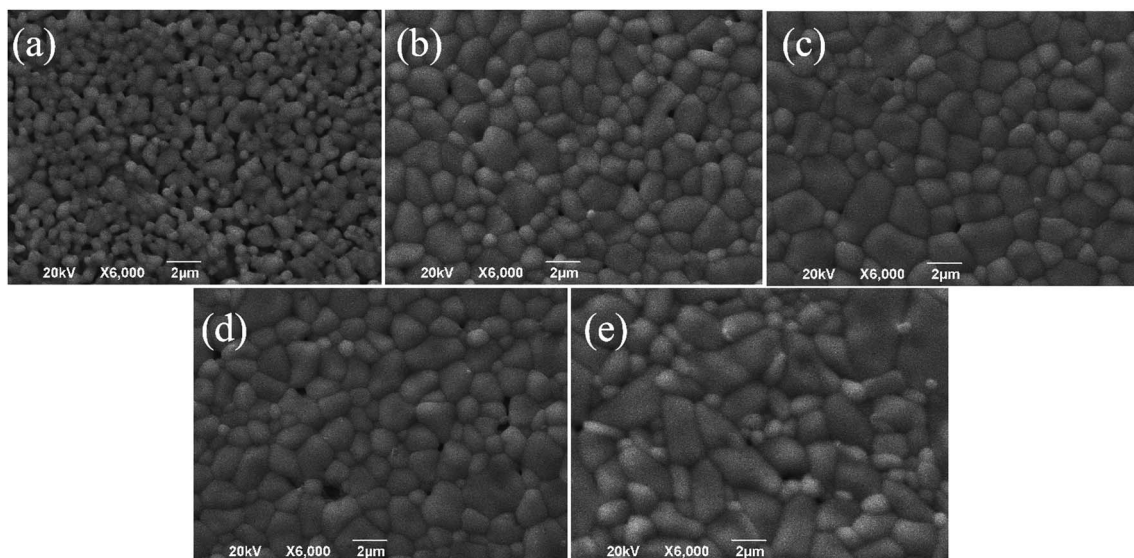


Fig. 3 Surface SEM micrographs of  $\text{MgNb}_2\text{O}_6-x$  wt% LMZBS ceramics sintered at  $925^\circ\text{C}$  (a)  $x = 0.1$ , (b)  $x = 0.5$ , (c)  $x = 1.0$ , (d)  $x = 1.5$ , (e)  $x = 2.0$ .

Raman models are provided by the Bilbao Crystallographic Server for analysis:<sup>30</sup>

$$\Gamma_{\text{Raman}} = 13A_g + 13A_u + 14B_{1g} + 14B_{1u} + 13B_{2g} + 13B_{2u} + 14B_{3g} + 14B_{3u} \quad (2)$$

Theoretically,  $\text{MgNb}_2\text{O}_6$  ceramic have 108 vibration modes. However, only several Raman modes could be observed due to

the interaction or overlapping. The bands in wavelength from  $200$  to  $250\text{ cm}^{-1}$  were assigned to the twisting vibration in and between chains; the bands in wavelength from  $250$  to  $400\text{ cm}^{-1}$  were attributed to the twisting vibration of octahedron; the bands in wavelength from  $400$  to  $1000\text{ cm}^{-1}$  were related to the stretching vibration of Nb–O bonds. Weak peak  $846\text{ cm}^{-1}$  corresponds to the antisymmetric stretching vibration mode of Nb–Ot of  $\text{NbO}_6$  octahedron in double chain plane (among them,

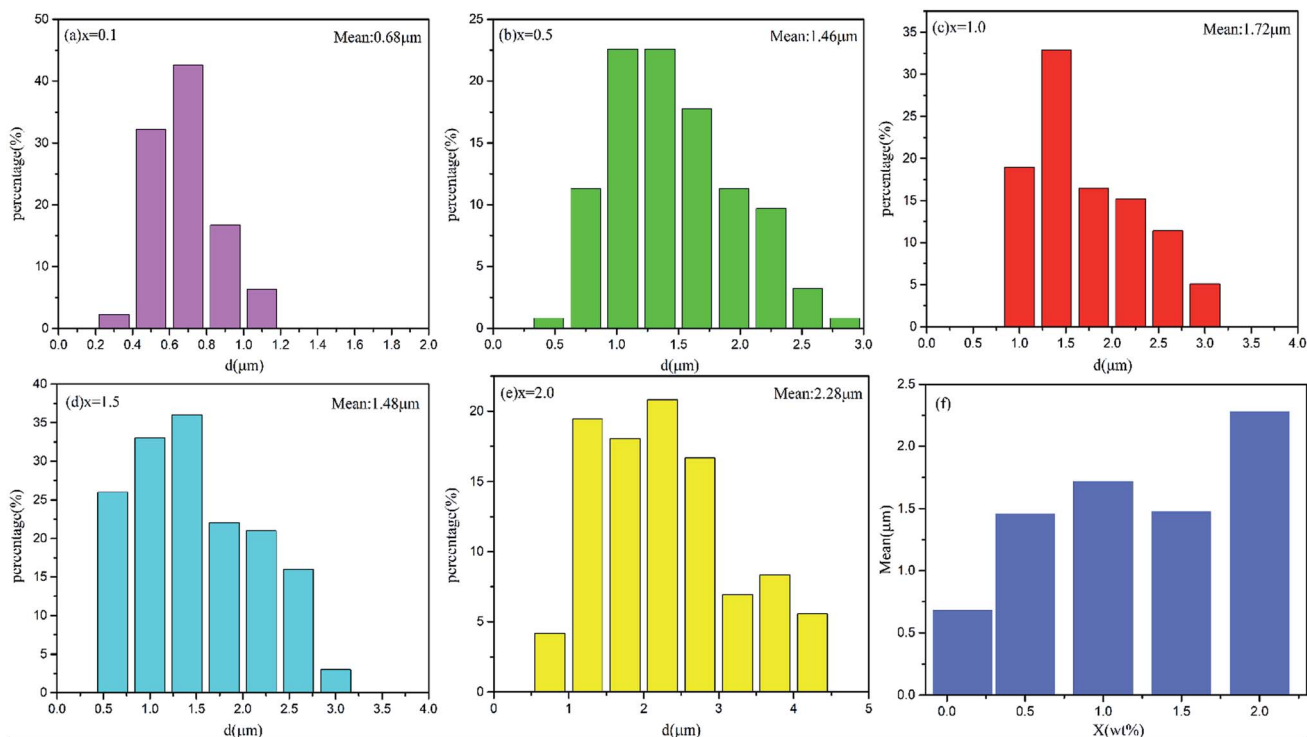


Fig. 4 The grain sizes distribution of  $\text{MgNb}_2\text{O}_6-x$  wt% LMZBS ( $x = 0.1, 0.5, 1.0, 1.5$  and  $2.0$ ) ceramics sintered at  $925^\circ\text{C}$ . (a–e) Grain sizes distribution, (f) mean grain size.



Ot represents an oxygen atom linked to a Nb atom and two Mg atoms), this is consistent with the Raman spectrum reported by Y. C. You *et al.*<sup>31</sup> It can be observed from Fig. 2 that no new Raman peak appears. By comparing the position of Raman peak, it is found that the additions of LMZBS have no influence on Raman spectrum.

### 3.2. Microstructure analysis

Fig. 3 and 4 show the SEM diagram and distribution of grain sizes of  $\text{MgNb}_2\text{O}_6$  ceramics sintered at 925 °C. LMZBS glass has a remarkable influence on the average grain size and density of  $\text{MgNb}_2\text{O}_6$  ceramics. In Fig. 3a, it can be intuitively seen that the grains are loose and irregular, and the average grain size was 0.68  $\mu\text{m}$ , which is related to low amount of LMZBS glass. With the amount of LMZBS glass increasing, the grains started to grow, as shown in Fig. 3b. When the doping amount reaches 1 wt%, uniform and dense microstructure with clear grain boundaries could be observed. The average grain size reached to 1.72  $\mu\text{m}$  and there was barely any hole. Because an appropriate amount of LMZBS glass will melt to form a liquid phase during sintering, which will make the grains of ceramic moist and thus promote the densification of ceramics. Nevertheless, with the further increase of doping amount, the grain grew abnormally and the average size of the grain is 1.48  $\mu\text{m}$ . From Fig. 3e, abnormal grains growth can be obviously observed. The average grain size increased to 2.28  $\mu\text{m}$ , and the grain boundary was indistinct, which may deteriorate the microwave dielectric characteristics. These results show that the proper amount of LMZBS glass can increase relative density and decrease porosity.

### 3.3. Dielectric characteristics analysis

Fig. 5 shows the apparent density of  $\text{MgNb}_2\text{O}_6$  ceramic with different doping amounts at different sintering temperatures. When the doping amount ranged from 0.1 wt% to 1.0 wt%, the density increased under same sintering temperature.<sup>32</sup> Finally,  $\text{MgNb}_2\text{O}_6$  ceramic with 1.0 wt% LMZBS glass at 925 °C had the

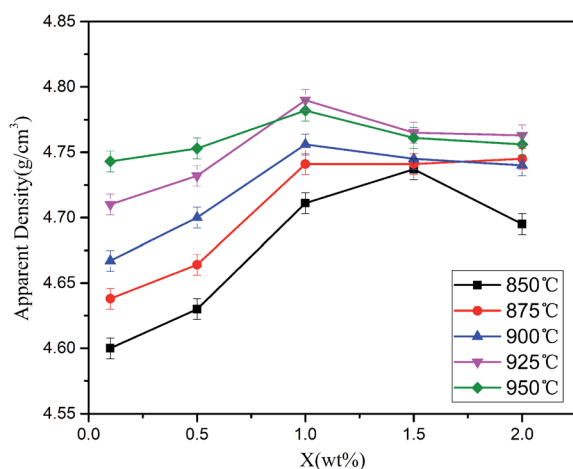


Fig. 5 Apparent densities of  $\text{MgNb}_2\text{O}_6-x$  wt% LMZBS ( $0.1 \leq x \leq 2.0$ ) ceramics sintered at different temperatures.

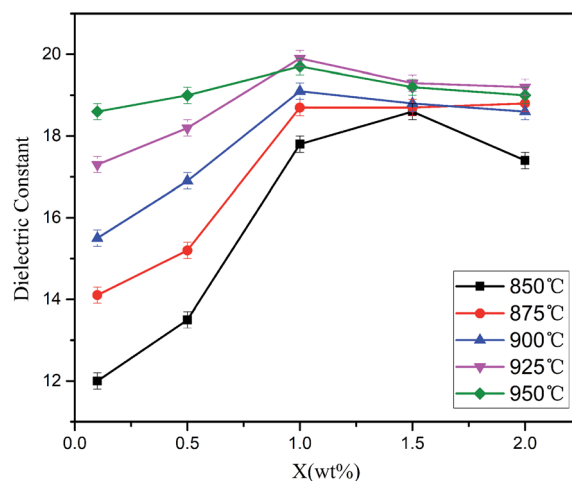


Fig. 6 The dielectric constant of  $\text{MgNb}_2\text{O}_6-x$  wt% LMZBS ( $0.1 \leq x \leq 2.0$ ) ceramics sintered at various temperatures for 5 h.

highest apparent density. This is attributed to the increase in liquid phase. However, with the further increase of the doping amount, the apparent density decreased slightly. This was because the excessive LMZBS addition led to excessive liquid phase, resulting in abnormal grain growth and porosity, which eventually led to the decrease in the density of  $\text{MgNb}_2\text{O}_6$  ceramic.

According to Fig. 6, it can be observed that when the doping amount is in the range of 0.1 wt% to 1.0 wt%, the dielectric constant is related to the doping proportion exhibiting a similar tendency as the apparent density. As known, second phase, molecular volume, structural characteristics, density and ionic polarizability affect the dielectric constant.<sup>33,34</sup> As shown in Fig. 1, there is no impurity in the ceramic system, so the influence of the second phase on the dielectric constant can be excluded. In this paper, apparent density is the primary factor impacting the dielectric constant. High density means low porosity and large dielectric constant. Therefore, dielectric constant is related to the density.

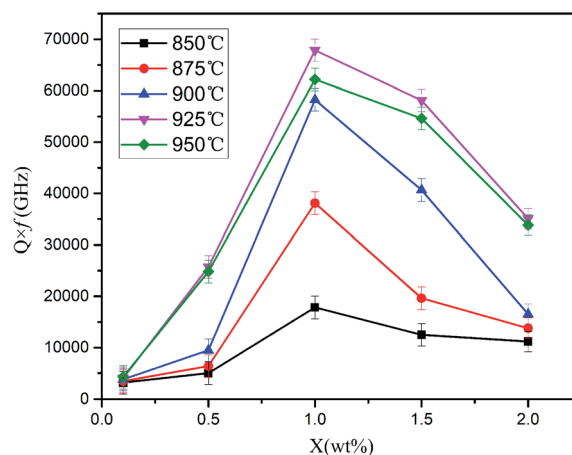


Fig. 7 The  $Q \times f$  values of  $\text{MgNb}_2\text{O}_6-x$  wt% LMZBS ( $0.1 \leq x \leq 2.0$ ) ceramics sintered at various temperatures.



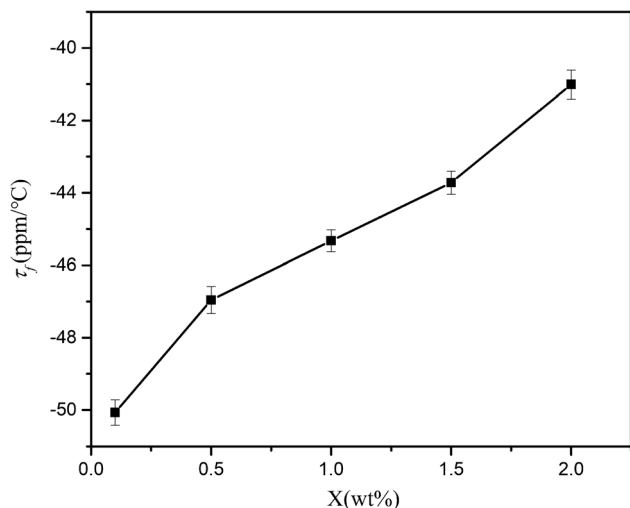


Fig. 8  $\tau_f$  values for the  $\text{MgNb}_2\text{O}_6-x$  wt% LMZBS ceramics sintered at 925 °C.

Fig. 7 demonstrates the  $Q \cdot f$  value of  $\text{MgNb}_2\text{O}_6$  ceramic under different sintering temperatures and different LMZBS amounts. The  $Q \cdot f$  value increased firstly until reaching the peak and decreased with the amount of LMZBS glass gradually increasing. Samples with same LMZBS amount got different  $Q \cdot f$  at different temperature and we can see that ceramic got the highest  $Q \cdot f$  at 925 °C. Besides, for the samples sintered at 925 °C with 1.0 wt% LMZBS glass, the optimal  $Q \cdot f$  value was 67 839 GHz. The results demonstrate that 925 °C is the optimization

sintering temperature for  $\text{MgNb}_2\text{O}_6$  ceramic in terms of densification and dielectric performance. In general, the dielectric loss is mainly composed of two modules: internal loss and external loss. Among them, the intrinsic loss is difficult to avoid, because it is the inherent nature of the material. However, external losses are affected by various factors, including second phase, porosity, grain boundaries, average grain size, and microstructure defects, *etc.*<sup>35,36</sup> XRD patterns show that there is no second phase, so the influence of secondary phase on  $Q \cdot f$  can be excluded. In this work, microwave dielectric loss is mainly affected by apparent density. With the increase of doping amount, the variation in  $Q \cdot f$  value are roughly similar to the change of apparent density. This is because the  $Q \cdot f$  value is impacted by the density.<sup>37,38</sup> Therefore, the proper amount of LMZBS glass can effectively improve the  $Q \cdot f$  value of  $\text{MgNb}_2\text{O}_6$  ceramic, which can make the dielectric ceramics have higher relative density and lower porosity.

Fig. 8 exhibits the  $\tau_f$  of  $\text{MgNb}_2\text{O}_6-x$  wt% LMZBS ( $x = 0.1, 0.5, 1.0, 1.5$  and  $2.0$ ) ceramics at optimal temperatures. It can be found that with the increase of glass addition,  $\tau_f$  value ranged from  $-50.7 \text{ ppm } ^\circ\text{C}^{-1}$  to  $-41.01 \text{ ppm } ^\circ\text{C}^{-1}$ . In general, the smaller the  $|\tau_f|$ , the better the thermal stability of dielectric ceramics.<sup>39</sup> In this work, the phase composition and crystal structure had no significant effect on  $\tau_f$  value. Therefore, the change of  $\tau_f$  value can be attributed to famous Lichtenecker empirical logarithmic rule:<sup>40</sup>

$$\tau_f = V_1\tau_{f_1} + V_2\tau_{f_2} \quad (3)$$

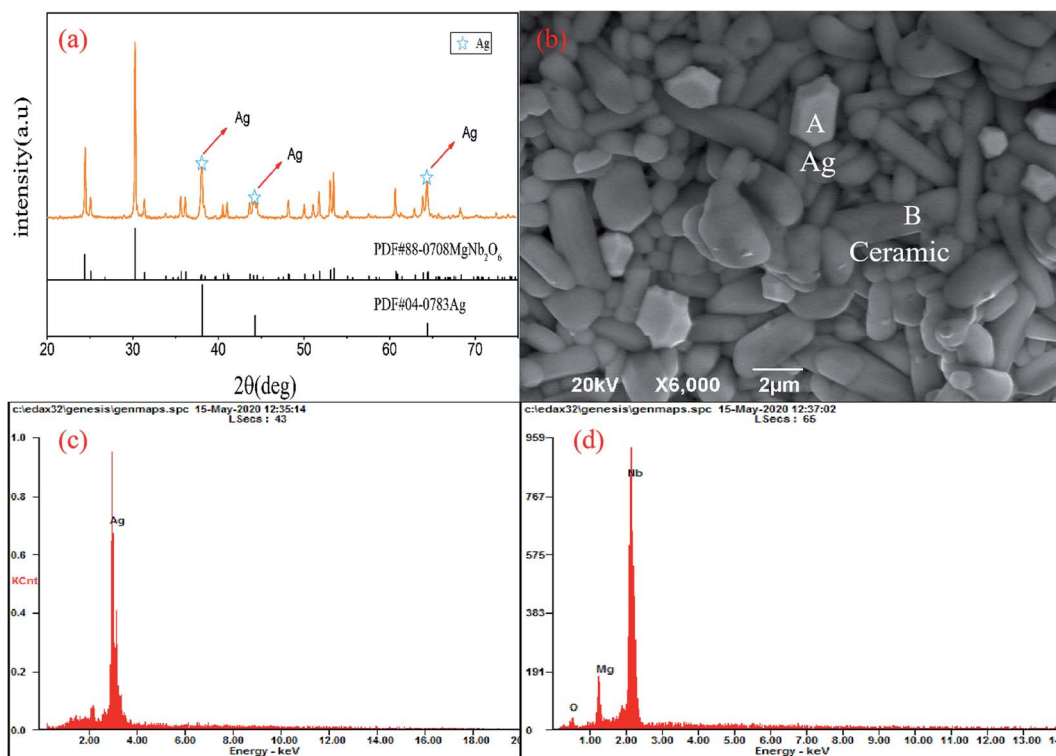


Fig. 9 XRD, SEM and EDX analysis of  $\text{MgNb}_2\text{O}_6$  ceramics doped with 1.0 wt% LMZBS and co-fired with 20 wt% Ag at 925 °C for 5 h. (a) XRD pattern, (b) back scattered electron images, (c) EDX analysis on A spot, and (d) EDX analysis on B spot.



Table 1 Comparison of microwave dielectric properties among MgNb<sub>2</sub>O<sub>6</sub> ceramics

| Material                         | Dopant                            | Temperature (°C) | $\epsilon_r$ | Q·f (GHz) | $\tau_f$ (ppm) | Co-fired with Ag | References                             |
|----------------------------------|-----------------------------------|------------------|--------------|-----------|----------------|------------------|--|
| MgNb <sub>2</sub> O <sub>6</sub> | —                                 | 1300             | 19.9         | 79 600    | −64.9          | No               | Pullar <i>et al.</i> <sup>19</sup>     |
| MgNb <sub>2</sub> O <sub>6</sub> | B <sub>2</sub> O <sub>3</sub>     | 1260             | 21.5         | 115 800   | −48            | No               | Huang <i>et al.</i> <sup>42</sup>      |
| MgNb <sub>2</sub> O <sub>6</sub> | CuO–B <sub>2</sub> O <sub>3</sub> | 1050             | 21.5         | 108 000   | −44            | No               | Tian Z. Q. <i>et al.</i> <sup>20</sup> |
| MgNb <sub>2</sub> O <sub>6</sub> | Fe <sub>2</sub> O <sub>3</sub>    | 1140             | 20.5         | 70 000    | −49            | No               | Hsu <i>et al.</i> <sup>43</sup>        |
| MgNb <sub>2</sub> O <sub>6</sub> | LMZBS                             | 925              | 19.7         | 67 839    | −41.01         | Yes              | This work                              |

where  $V_1$ ,  $V_2$  and  $\tau_{f_1}$ ,  $\tau_{f_2}$  are the volume fractions and  $\tau_f$  values of pure MgNb<sub>2</sub>O<sub>6</sub> and LMZBS, respectively ( $V_1 + V_2 = 1$ ). On the one hand,  $\tau_f$  value of pure MgNb<sub>2</sub>O<sub>6</sub> ceramic is  $-64.9 \text{ ppm } ^\circ\text{C}^{-1}$ .<sup>19</sup> On the other hand, low-melting glass LMZBS have negative  $\tau_f$  value,<sup>41</sup> which may explain the reason why the  $\tau_f$  value changed slightly. Adding  $\tau_f$  compensation materials have proved to be an effective method to adjust the  $\tau_f$  to near zero. Therefore, in the next step, we may choose the CaTiO<sub>3</sub> (+800 ppm  $^\circ\text{C}^{-1}$ ) and SrTiO<sub>3</sub> (+1600 ppm  $^\circ\text{C}^{-1}$ ) to adjust  $\tau_f$  for the MgNb<sub>2</sub>O<sub>6</sub> ceramic.

It is imperative to research the chemical compatibility of the MgNb<sub>2</sub>O<sub>6</sub> ceramics with silver for practical LTCC applications. Fig. 9a exhibits the XRD pattern of the 1.0 wt% LMZBS-doped MgNb<sub>2</sub>O<sub>6</sub> ceramics co-fired with 20 wt% Ag powders sintered at 925 °C. No chemical reaction occurred between MgNb<sub>2</sub>O<sub>6</sub> ceramics and Ag. Fig. 9b–d show the back scattered electron images and elements distribution of the fracture surface. The EDX analysis proves that there is no reaction between ceramic and silver. The whole experimental results confirm that the 1.0 wt% LMZBS-doped MgNb<sub>2</sub>O<sub>6</sub> ceramic can be compatible with Ag. Besides, the comparison between this work and previous literature is listed in Table 1. It can be observed that the MgNb<sub>2</sub>O<sub>6</sub> ceramics doped with LMZBS exhibited chemical compatibility with silver electrodes without deteriorating microwave dielectric properties, which makes MgNb<sub>2</sub>O<sub>6</sub> ceramics as promising material for LTCC applications.

## 4. Conclusions

MgNb<sub>2</sub>O<sub>6</sub> ceramics doped with LMZBS glass were prepared by solid phase reaction process. The effects of LMZBS amount on the phase composition, microstructure, grain growth, apparent density, chemical compatibility with Ag and microwave properties of ceramics were studied. Raman spectra and XRD demonstrate single columbite MgNb<sub>2</sub>O<sub>6</sub> phase. The scanning electron microscope (SEM) results indicated that the homogeneous and dense microstructure appeared at 925 °C. The relative density and  $\epsilon_r$  have similar variation tendency. With the increase of LMZBS amount,  $\tau_f$  value shifted towards positive direction. Particularly, the MgNb<sub>2</sub>O<sub>6</sub>–1.0 wt% LMZBS ceramic obtained at 925 °C possessed optimum microwave dielectric characteristics:  $\epsilon_r = 19.7$ ,  $Q \cdot f = 67\,839 \text{ GHz}$ ,  $\tau_f = -41.01 \text{ ppm } ^\circ\text{C}^{-1}$ . Meanwhile, XRD pattern and EDX elements analysis proved that the MgNb<sub>2</sub>O<sub>6</sub> ceramic showed excellent chemical compatibility with Ag, which confirmed the applicability of MgNb<sub>2</sub>O<sub>6</sub> ceramic in LTCC.

## Conflicts of interest

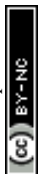
There are no conflicts to declare.

## References

- Q. Liao, L. Li, X. Ren, X. Yu, D. Guo and M. Wang, A low sintering temperature low loss microwave dielectric material ZnZrNb<sub>2</sub>O<sub>8</sub>, *J. Am. Ceram. Soc.*, 2012, **95**(11), 3363–3365.
- M. T. Sebastian and H. Jantunen, High Temperature Cofired Ceramic (HTCC), Low Temperature Cofired Ceramic (LTCC), and Ultralow Temperature Cofired Ceramic (ULTCC) Materials, *Microwave Materials and Applications 2V Set*, 2017, pp. 355–425.
- W. Wang, L. Li, S. Xiu, B. Shen and J. Zhai, Microwave dielectric properties of (Mg<sub>0.4</sub>Zn<sub>0.6</sub>)<sub>2</sub>SiO<sub>4</sub>–CaTiO<sub>3</sub> ceramics sintered with Li<sub>2</sub>CO<sub>3</sub>–H<sub>3</sub>BO<sub>3</sub> for LTCC technology, *J. Alloys Compd.*, 2015, **639**, 359–364.
- G. Wang, H. Zhang, C. Liu, H. Su, L. Jia, J. Li and G. Gan, Low-Temperature Sintering Li<sub>3</sub>Mg<sub>1.8</sub>Ca<sub>0.2</sub>NbO<sub>6</sub> Microwave Dielectric Ceramics with LMZBS Glass, *J. Electron. Mater.*, 2018, **47**(8), 4672–4677.
- D. Zhou, L. X. Pang, D. W. Wang, C. Li, B. B. Jin and I. M. Reaney, High permittivity and low loss microwave dielectrics suitable for 5G resonators and low temperature co-fired ceramic architecture, *J. Mater. Chem. C*, 2017, **5**(38), 10094–10098.
- H. Ren, M. Dang, H. Wang, T. Xie, S. Jiang, H. Lin and L. Luo, Sintering behavior and microwave dielectric properties of B<sub>2</sub>O<sub>3</sub>–La<sub>2</sub>O<sub>3</sub>–MgO–TiO<sub>2</sub> based glass-ceramic for LTCC applications, *Mater. Lett.*, 2018, **210**, 113–116.
- G. G. Yao, P. Liu and H. W. Zhang, Novel Series of Low-Firing Microwave Dielectric Ceramics: Ca<sub>5</sub>A<sub>4</sub>(VO<sub>4</sub>)<sub>6</sub>(A<sup>2+</sup> = Mg, Zn), *J. Am. Ceram. Soc.*, 2013, **96**(6), 1691–1693.
- H. Zhou, H. Wang, Y. Chen, K. Li and X. Yao, Low temperature sintering and microwave dielectric properties of Ba<sub>3</sub>Ti<sub>5</sub>Nb<sub>6</sub>O<sub>28</sub> ceramics with BaCu(B<sub>2</sub>O<sub>3</sub>)<sub>2</sub> additions, *Mater. Chem. Phys.*, 2009, **113**(1), 1–5.
- J. Xiang, Z. Xie, Y. Huang and H. Xiao, Synthesis of Ti(C, N) ultrafine powders by carbothermal reduction of TiO<sub>2</sub> derived from sol–gel process, *J. Eur. Ceram. Soc.*, 2000, **20**(7), 933–938.
- Y. S. Hong, H. B. Park and S. J. Kim, Preparation of Pb(Mg<sub>13</sub>Nb<sub>23</sub>)O<sub>3</sub> powder using a citrate-gel derived



- columbite  $\text{MgNb}_2\text{O}_6$  precursor and its dielectric properties, *J. Eur. Ceram. Soc.*, 1998, **18**(6), 613–619.
- 11 S. Ananta, Phase and morphology evolution of magnesium niobate powders synthesized by solid-state reaction, *Mater. Lett.*, 2004, **58**(22–23), 2781–2786.
  - 12 G. Wang, H. Zhang, X. Huang, F. Xu, G. Gan, Y. Yang and L. Jin, Correlations between the structural characteristics and enhanced microwave dielectric properties of V-modified  $\text{Li}_3\text{Mg}_2\text{NbO}_6$  ceramics, *Ceram. Int.*, 2018, **44**(16), 19295–19300.
  - 13 G. Wang, H. Zhang, C. Liu, H. Su, J. Li, X. Huang and F. Xu, Low temperature sintering and microwave dielectric properties of novel temperature stable  $\text{Li}_3\text{Mg}_2\text{NbO}_6\text{-}0.1\text{TiO}_2$  ceramics, *Mater. Lett.*, 2018, **217**, 48–51.
  - 14 Y. Liao, F. Xu, D. Zhang, T. Zhou, Q. Wang, X. Wang and H. Zhang, Low temperature firing of  $\text{Li}_{0.43}\text{Zn}_{0.27}\text{Ti}_{0.13}\text{Fe}_{2.17}\text{O}_4$  ferrites with enhanced magnetic properties, *J. Am. Ceram. Soc.*, 2015, **98**(8), 2556–2560.
  - 15 E. A. Nenasheva and N. F. Kartenko, Low-sintering ceramic materials based on  $\text{Bi}_2\text{O}_3\text{-ZnO-Nb}_2\text{O}_5$  compounds, *J. Eur. Ceram. Soc.*, 2006, **26**(10–11), 1929–1932.
  - 16 G. Wang, D. Zhang, Y. Lai, X. Huang, Y. Yang, G. Gan and L. Jin, Ultralow loss and temperature stability of  $\text{Li}_3\text{Mg}_2\text{NbO}_6\text{-xLiF}$  ceramics with low sintering temperature, *J. Alloys Compd.*, 2019, **782**, 370–374.
  - 17 R. C. Pullar, The synthesis, properties, and applications of columbite niobates ( $\text{M}^{2+}\text{Nb}_2\text{O}_6$ ): a critical review, *J. Am. Ceram. Soc.*, 2009, **92**(3), 563–577.
  - 18 Y. C. Liou, M. H. Weng and C. Y. Shiue,  $\text{CaNb}_2\text{O}_6$  ceramics prepared by a reaction-sintering process, *Mater. Sci. Eng., B*, 2006, **133**(1–3), 14–19.
  - 19 R. C. Pullar, J. D. Breeze and N. M. Alford, Characterization and microwave dielectric properties of  $\text{M}^{2+}\text{Nb}_2\text{O}_6$  ceramics, *J. Am. Ceram. Soc.*, 2005, **88**(9), 2466–2471.
  - 20 Z. Q. Tian and L. Lin, Low temperature sintering and microwave dielectric properties of  $\text{MgNb}_2\text{O}_6$  ceramics, *J. Mater. Sci.: Mater. Electron.*, 2009, **20**(9), 867–871.
  - 21 G. Wang, H. Zhang, C. Liu, H. Su, L. Jia, J. Li and G. Gan, Low-Temperature Sintering  $\text{Li}_3\text{Mg}_{1.8}\text{Ca}_{0.2}\text{NbO}_6$  Microwave Dielectric Ceramics with LMZBS Glass, *J. Electron. Mater.*, 2018, **47**(8), 4672–4677.
  - 22 K. Manu and M. T. Sebastian, Tape casting of low permittivity Wesselsite–Glass composite for LTCC based microwave applications, *Ceram. Int.*, 2016, **42**(1), 1210–1216.
  - 23 K. N. Singh and P. K. Bajpai, Synthesis, characterization and dielectric relaxation of phase pure columbite  $\text{MgNb}_2\text{O}_6$ : optimization of calcination and sintering, *Phys. B*, 2010, **405**(1), 303–312.
  - 24 K. Sreedhar and A. Mitra, Formation of lead magnesium niobate perovskite from  $\text{MgNb}_2\text{O}_6$  and  $\text{Pb}_3\text{Nb}_2\text{O}_8$  precursors, *Mater. Res. Bull.*, 1997, **32**(12), 1643–1649.
  - 25 A. Belous, O. Ovchar, B. Jancar and J. Bezjak, The effect of non-stoichiometry on the microstructure and microwave dielectric properties of the columbites  $\text{A}^{2+}\text{Nb}_2\text{O}_6$ , *J. Eur. Ceram. Soc.*, 2007, **27**(8–9), 2933–2936.
  - 26 S. Ananta, R. Brydson and N. W. Thomas, Synthesis, formation and characterisation of  $\text{MgNb}_2\text{O}_6$  powder in a columbite-like phase, *J. Eur. Ceram. Soc.*, 1999, **19**(3), 355–362.
  - 27 G. Wang, D. Zhang, X. Huang, Y. Rao, Y. Yang, G. Gan and C. Liu, Crystal structure and enhanced microwave dielectric properties of  $\text{Ta}^{5+}$  substituted  $\text{Li}_3\text{Mg}_2\text{NbO}_6$  ceramics, *J. Am. Ceram. Soc.*, 2020, **103**(1), 214–223.
  - 28 G. Wang, D. Zhang, F. Xu, X. Huang, Y. Yang, G. Gan and L. Jin, Correlation between crystal structure and modified microwave dielectric characteristics of  $\text{Cu}^{2+}$  substituted  $\text{Li}_3\text{Mg}_2\text{NbO}_6$  ceramics, *Ceram. Int.*, 2019, **45**(8), 10170–10175.
  - 29 X. Shi, H. Zhang, D. Zhang, F. Xu, Y. Zheng, G. Wang and L. Jia, Correlation between structure characteristics and dielectric properties of  $\text{Li}_2\text{Mg}_3\text{-xCu}_x\text{TiO}_6$  ceramics based on complex chemical bond theory, *Ceram. Int.*, 2019, **45**(17), 23509–23514.
  - 30 E. Kroumova, M. I. Aroyo, J. M. Perez-Mato, A. Kirov, C. Capillas, S. Ivantchev and H. Wondratschek, Bilbao crystallographic server: useful databases and tools for phase-transition studies, *Phase Transitions A Multinatl. J.*, 2003, **76**(1–2), 155–170.
  - 31 Y. C. You, H. L. Park, Y. G. Song, H. S. Moon and G. C. Kim, Stable phases in the  $\text{MgO-Nb}_2\text{O}_5$  system at 1250°C, *J. Mater. Sci. Lett.*, 1994, **13**(20), 1487–1489.
  - 32 G. Wang, D. Zhang, G. Gan, Y. Yang, Y. Rao, F. Xu and L. Jin, Synthesis, crystal structure and low loss of  $\text{Li}_3\text{Mg}_2\text{NbO}_6$  ceramics by reaction sintering process, *Ceram. Int.*, 2019, **45**(16), 19766–19770.
  - 33 Q. Liao, L. Li, X. Ren, X. Yu, Q. Meng and W. Xia, A new microwave dielectric material  $\text{Ni}_{0.5}\text{Ti}_{0.5}\text{NbO}_4$ , *Mater. Lett.*, 2012, **89**, 351–353.
  - 34 E. S. Kim, D. H. Kang, J. M. Yang, H. S. Shin, N. I. Zahari and H. Ohsato, Crystal structure and dielectric properties of  $\text{Ca}_{0.85}\text{Nd}_{0.1}\text{TiO}_3\text{-LnAlO}_3$  ceramics, *IEEE Trans. Ultrason. Ferroelectrics Freq. Contr.*, 2008, **55**(5), 1075–1080.
  - 35 M. Guo, S. Gong, G. Dou and D. Zhou, A new temperature stable microwave dielectric ceramics:  $\text{ZnTiNb}_2\text{O}_8$  sintered at low temperatures, *J. Alloys Compd.*, 2011, **509**(20), 5988–5995.
  - 36 S. J. Penn, N. M. Alford, A. Templeton, X. Wang, M. Xu, M. Reece and K. Schrapel, Effect of porosity and grain size on the microwave dielectric properties of sintered alumina, *J. Am. Ceram. Soc.*, 1997, **80**(7), 1885–1888.
  - 37 S. H. Yoon, G. K. Choi, D. W. Kim, S. Y. Cho and K. S. Hong, Mixture behavior and microwave dielectric properties of  $(1-x)\text{CaWO}_4\text{-xTiO}_2$ , *J. Eur. Ceram. Soc.*, 2007, **27**(8–9), 3087–3091.
  - 38 Z. Fang, B. Tang, F. Si, E. Li, H. Yang and S. Zhang, Phase evolution, structure and microwave dielectric properties of  $\text{Li}_{2+x}\text{Mg}_3\text{SnO}_6$  ( $x=0.00\text{--}0.12$ ) ceramics, *Ceram. Int.*, 2017, **43**(16), 13645–13652.
  - 39 P. Zhang, M. Yang and M. Xiao, Sintering behavior, crystalline structure and microwave dielectric properties of  $\text{Li}_2(\text{Ni}_{1-x}\text{Mg}_x)_3\text{TiO}_6$  ( $0\leq x\leq 1$ ) ceramics, *Ceram. Int.*, 2018, **44**(17), 21607–21612.
  - 40 L. X. Pang, H. Wang, D. Zhou and X. Yao, A new temperature stable microwave dielectric with low-firing temperature in



- $\text{Bi}_2\text{MoO}_6\text{-TiO}_2$  system, *J. Alloys Compd.*, 2010, **493**(1–2), 626–629.
- 41 T. Joseph, M. T. Sebastian, H. Sreemoolanadhan and V. K. Sree Nageswari, Effect of glass addition on the microwave dielectric properties of  $\text{CaMgSi}_2\text{O}_6$  ceramics, *Int. J. Appl. Ceram. Technol.*, 2010, **7**, E98–E106.
- 42 C. L. Huang and K. H. Chiang, Improved high-Q microwave dielectric material using  $\text{B}_2\text{O}_3$ -doped  $\text{MgNb}_2\text{O}_6$  ceramics, *Mater. Sci. Eng., A*, 2008, **474**(1–2), 243–246.
- 43 C. H. Hsu, C. F. Tseng and C. L. Huang, Microwave dielectric properties of  $\text{MgNb}_2\text{O}_6$  ceramics with  $\text{Fe}_2\text{O}_3$  additives, *Jpn. J. Appl. Phys.*, 2005, **44**(11R), 8043.
- 44 S. George, P. S. Anjana, V. N. Deepu, P. Mohanan and M. T. Sebastian, Low-temperature sintering and microwave dielectric properties of  $\text{Li}_2\text{MgSiO}_4$  ceramics, *J. Am. Ceram. Soc.*, 2009, **92**(6), 1244–1249.
- 45 H. H. Guo, D. Zhou, C. Du, P. J. Wang, W. F. Liu, L. X. Pang and S. Trukhanov, Temperature stable  $\text{Li}_2\text{Ti}_{0.75}(\text{Mg}_{1/3}\text{Nb}_{2/3})_{0.25}\text{O}_3$ -based microwave dielectric ceramics with low sintering temperature and ultra-low dielectric loss for dielectric resonator antenna applications, *J. Mater. Chem. C*, 2020, **8**(14), 4690–4700.
- 46 H. H. Guo, D. Zhou, L. X. Pang and Z. M. Qi, Microwave dielectric properties of low firing temperature stable scheelite structured  $(\text{Ca}, \text{Bi})(\text{Mo}, \text{V})\text{O}_4$  solid solution ceramics for LTCC applications, *J. Eur. Ceram. Soc.*, 2019, **39**(7), 2365–2373.

